applied sciences

MDPI

Article

Investigating the Role of Microclimate and Microorganisms in the Deterioration of Stone Heritage: The Case of Rupestrian Church from Jac, Romania

Dorina Camelia Ilieș [1], Andrei-Ionuț Apopei [2], Cristina Mircea [3], Alexandru Ilieș [1], Tudor Caciora [1,*], Berdenov Zharas [4], Lucian Barbu-Tudoran [5], Nicolaie Hodor [6], Alexandru Turza [7], Ana Cornelia Pereș [8], Thowayeb H. Hassan [9,10], Bahodirhon Safarov [11] and Ioan-Cristian Noje [12]

1 Department of Geography, Tourism and Territorial Planning, Faculty of Geography, Tourism and Sport, University of Oradea, 1 Universitatii Street, 410087 Oradea, Romania; dilies@uoradea.ro (D.C.I.); ilies@uoradea.ro (A.I.)
2 Department of Geology, Faculty of Geography and Geology, "Alexandru Ioan Cuza" University of Iași, 700505 Iași, Romania; andrei.apopei@uaic.ro
3 Department of Molecular Biology and Biotechnology, Babes, Bolyai University, 1 M. Kogalniceanu St., 400084 Cluj-Napoca, Romania; cristina.mircea@ubbcluj.ro
4 Faculty of Science, L.N. Gumilyov Eurasian National University, 2 Satpayev Street, Nur-Sultan 010008, Kazakhstan; berdenov_zhg_1@enu.kz
5 Electron Microscopy Center "Prof. C. Craciun", Faculty of Biology & Geology, Babes-Bolyai University, 5-7 Clinicilor Str., 400006 Cluj-Napoca, Romania; lucian.barbu@itim-cj.ro
6 Department of Physical and Technical Geography, Faculty of Geography, Babes-Bolyai University, 5-6 Clinicilor Street, 400006 Cluj-Napoca, Romania; nicolaie.hodor@ubbcluj.ro
7 National Institute for R&D of Isotopic and Molecular Technologies, 67-103 Donat Street, 400293 Cluj-Napoca, Romania; alexandru.turza@itim-cj.ro
8 Department of Environmental Engineering, Faculty of Environmental Protection, University of Oradea, Magheru Street 26, 410087 Oradea, Romania; peresana35@yahoo.com
9 Social Studies Department, College of Arts, King Faisal University, Al Ahsa 31982, Saudi Arabia; thassan@kfu.edu.sa
10 Tourism Studies Department, Faculty of Tourism and Hotel Management, Helwan University, Cairo 12612, Egypt
11 Department of Digital Economy, Samarkand Branch of Tashkent State University of Economics, Samarkand 140105, Uzbekistan; safarovb@rambler.ru
12 Doctoral School in Geography, University of Oradea, 1 Universitatii Street, 410087 Oradea, Romania; nojecristian@yahoo.com
* Correspondence: tudor.caciora@yahoo.com; Tel.: +40-740941144

Abstract: Natural stone can undergo disaggregation from various causes, including physical actions such as freeze–thaw cycles, temperature and humidity variations, chemical actions such as the solubilization of minerals by organic and inorganic acids, as well as biological actions due to the colonization of organisms that can produce biocorrosion and biomineralization. This research investigates the impact of microclimatic conditions and microbial activity on the physical and chemical integrity of stone heritage, particularly the biodeterioration caused by fungi in the case of a Romanian rock church. Various analytical techniques were employed, including macroscopic and optical microscopy, Raman spectroscopy, X-ray diffraction, and culture-based identification methods, to characterize the mineral composition and microbial contamination of the rock samples. The analyses revealed that the sandstone consists primarily of quartz (over 90%), muscovite (5–10%), and feldspars. The identified fungi included *Cladosporium herbarium*, *Aspergillus niger*, and *Mortierella hyalina*. The SEM images showed fungal hyphae and spores within the kaolinite–illite matrix, indicating significant microbial colonization and its role in rock deterioration. Additionally, microclimatic data collected over a 12-week period highlighted the substantial fluctuations in temperature and relative humidity within the church, which contribute to the physical and chemical weathering of the stone. This study also noted high levels of particulate matter ($PM_{2.5}$ and PM_{10}) and volatile organic compounds, which can exacerbate microbial growth and stone decay. The comprehensive analysis underscores the need

Citation: Ilieș, D.C.; Apopei, A.-I.; Mircea, C.; Ilieș, A.; Caciora, T.; Zharas, B.; Barbu-Tudoran, L.; Hodor, N.; Turza, A.; Pereș, A.C.; et al. Investigating the Role of Microclimate and Microorganisms in the Deterioration of Stone Heritage: The Case of Rupestrian Church from Jac, Romania. *Appl. Sci.* **2024**, *14*, 8136. https://doi.org/10.3390/app14188136

Academic Editor: António Manuel Santos Carriço Portugal

Received: 22 July 2024
Revised: 4 September 2024
Accepted: 5 September 2024
Published: 10 September 2024

for targeted preservation strategies that consider both microclimatic factors and microbial colonization to effectively conserve stone heritage sites, ensuring their longevity and structural integrity.

Keywords: stone heritage; microorganisms; biodeterioration; X-ray diffraction; Raman spectroscopy; preservation; conservation; mineralogical composition

1. Introduction

The cultural heritage built with stone support is extremely sensitive to degradations induced by microclimate and fungi, which can lead to physical weakening and discoloration of the materials, as well as their mechanical exfoliation through the penetration of fungi and the production of organic acids [1–4]. Thus, for cultural heritage elements located both in the external and internal environment, the study of the colonizing microbial community, which is very sensitive to climate and environmental changes, can be an effective indicator for monitoring the risks to which they are subjected [5–9]. Natural stone, found both in the interior and exterior environment, is subject to deterioration [10,11]. Microorganisms (especially lithobionts) thrive, grow, and develop, even in extremely harsh conditions (variations in microclimatic parameters; pronounced day/night and seasonal variations; environment with low nutrient and water content). Thus, it can be mentioned that physical damage (materialized by aesthetic alterations at the level of the rock surface, especially due to pigments and biofilms generated by microorganisms) chemical damage (biocorrosion and biomineralization processes, erosion, discoloration) due to some organic and inorganic acids; chelating agents enzymes, and extracellular polymeric substances produced by microbial metabolisms, especially in temperate and humid climate conditions [10,12,13]; and structural erosion of the rock is generated by the penetration of filamentous fungi (e.g., *Streptomycetes*, *Alternaria*, *Cladosporium*, *Ulocladium*, *Epicoccum*, etc.) [12].

The natural stone support can be negatively affected over time by weathering processes, with the disaggregation and alteration of the rock material, generally due to the action of environmental and anthropogenic factors, as well as due to the action of colonizing microorganisms. They can produce acids that can lead to crystalline aggression, with dissolution at the level of the component minerals (e.g., carbonates, silicates, phosphates, etc.). In the case of calcareous and siliceous rocks, the dissolution of calcite through the action of microorganisms is a process with dire consequences (sulfur oxidizers dissolve calcite in calcareous rocks and can generate gypsum crusts). On siliceous rocks, despite quartz being a more resistant mineral, calcite's vulnerability disrupts the stone structure's integrity [14].

Biopitting phenomena can also occur (especially on calcareous rocks and marbles). Sometimes, the formation of secondary minerals and mineral and biotic crusts is observed, with colored patinas on certain surfaces [15–18].

Biodeterioration is due to some phototrophic–heterotrophic communities, which install subaerial-mixed biofilms built from extracellular polymers (EPSs) (such as polysaccharides, lipids, proteins, nucleic acids, pigments, and enzymes), nutrients, and organic and inorganic compounds captured from the external environment (dust, pollen, remains of grass and leaves, bird excrement, mineral components of the stone) [19] that exist in the complex conditions of the natural stone system (external/internal climatic conditions, environmental factors, bioreceptivity of the rocks). The latter indicates the ability of the stone to retain and be a substrate for organisms depending on its mineralogical–petrographic characteristics and physical–chemical–mechanical properties, among which can be mentioned the porosity, roughness, permeability, pH of the substrate (alkaline rocks are more susceptible to fungal attacks than acid rocks), orientation and design of the artifact concerning the dominant direction of the wind, exposure to precipitation, and lack of prevention and conservation strategies [18]. On limestone in particular, types of fungi such as *Aspergillus*, *Cladosporium herbarium*, and *Alternaria tenuissima* biodegrade the stone through the cryp-

toendolithic growth of the species in specific microclimatic conditions [20]. The studies by Saleh et al. [21], El-Badry et al. [22], and El-Sayed and Maky [23] highlight the importance of experimental approaches in the consolidation and protection of sandstone artifacts, utilizing various analytical techniques such as petrography, scanning electron microscopy (SEM), X-ray diffraction (XRD), and energy-dispersive X-ray spectroscopy (EDXS) to assess the effects of aging and treatment processes on sandstone petroglyphs at Sarabit El Khadem and Wadi Hammamat in Egypt.

Multiple damages also occur due to the fungal hyphae penetrating inside the stone, constituting transport paths for water, organic compounds, and nutrients with the release of acids, thus facilitating the colonization of microorganisms in the internal part of the rock, associated with hyphae contraction, expansion processes, polysaccharides, the freeze–thaw of infiltrated water, etc. [24]. The physical and chemical degradation processes generate the formation of pores and cracks in the rock mass, which can intensify the actions of the biological factor, with the resumption and even intensification of the physical–chemical processes [25].

In temperate climates, bacteria and fungi are highlighted as important agents of weathering and altering natural stone. Bacteria, with the most common species being *Arthrobacter* sp., *Bacillus* sp., *Micrococcus* sp., *Pseudomonas* sp., *Streptomyces* sp., and *Thiobacillus* sp., are colonies that can be affected by fluctuating environmental and climatic factors (wind, rain, relative humidity, temperature, particulate matter, pollutants, etc.) as well as stone bioreceptivity [5].

The ecological group of fungi colonizing natural stone is characterized by the formation of thick, pigmented church walls that are easily adaptable to climatic and environmental conditions, facilitating water retention, with an important role in reducing desiccation and increasing adhesion. Fungal genera commonly isolated from stone artifacts include *Alternaria* sp., *Aspergillus* sp., *Cladosporium* sp., *Penicillium* sp., *Rhizopus* sp., and *Trichoderma* sp. [26–29]. Dematiaceous fungi, including genera such as *Aureobasidium*, *Coniosporium*, *Exophiala*, *Hortaea*, *Knuffia*, and *Phaeococcomyces*, for arid and semi-arid environments, respectively, and filamentous species from the genera *Alternaria*, *Cladosporium*, *Ulocladium*, and *Epicoccum* in temperate and humid environment conditions, respectively [18,30,31].

Black meristematic fungi (e.g., *Hortaea*, *Sarcinomyces*, *Exophiala*, *Knufiaspp Aureobasidium pullulans*) are melanized colonies developed on natural stone [11,16,27,32,33]. In the analyses carried out in various studies, white marble can be colonized by the genera *Ascomycota Cladophialophora*, *Devriesia*, *Knufia*, *Lithophila*, and *Vermiconia*, which were identified as dominant [18,34–36]. Aesthetic changes due to the extracellular pigments synthesized and excreted by black fungi lead to various colors, the installation of patina on the rock, etc., especially due to melanin; sometimes, however, melanin can also act as a protector against harmful radiation from the environment (UV radiation, X-rays and γ-rays, and chemical stress/stress factors).

Cyanobacteria can also be frequently found on monuments with natural stone supports; they are very adaptable to conditions of very high temperature (T) and a high degree of drying or pronounced humidity (e.g., India or Bangladesh). Certain species of cyanobacteria that dominate these biofilms develop survival strategies by secreting a thick sheath of EPS, rich in pigments (scytonemin and amino acids) that protect against very intense UV solar radiation and against drying [37]. In the case of stone colonization by cyanobacteria in conditions of high humidity, the generated biofilms become greenish in color from black/brown and attack the minerals in the stone's composition for nutrition, leading to aesthetic changes and its deterioration [37].

The current study aims to identify the possible dangers the integrity of an atypical cultural heritage element is subject to, namely a rupestrian church from the 11th–14th century, with a view to future conservation and a better understanding of it. Such case studies have been researched before: the research studies by Mang et al. [38] and Cardellicchio et al. [39] explore the impact of fungal contamination and biopatina formation on the rupestrian churches in Matera, Italy, highlighting the effectiveness of treatment methods,

including the use of glycoalkaloids, to manage microbial growth and preserve the structural integrity of these historical sites. In our case, the mineralogical composition of the supporting rock and the identification of the associated microorganisms were considered in order to understand the mechanisms of damage and the effects on the structure and surface of the rock. These were corroborated with a determination of the internal and external microclimatic characteristics of the rock church, including T, relative humidity (RH), CO_2, $PM_{2.5}$, PM_{10}, VOC, and HCHO, to assess their impact on the conservation of the monument and the development of fungal colonies. All of these have as their final goal the establishment of strategies, based on the data obtained, that take into account the prevention of damage induced by microclimate and bacteriological microflora to ensure the long-term preservation of the historical monument.

2. Materials and Methods

The rupestrian church from Jac is located in the northeastern part of Viile Jacului hamlet, Creaca commune, Sălaj County, Romania (Figure 1). The church is part of the cult edifices category and is included both in the list of historical monuments in Sălaj County and in the National Archaeological Repertory. It was constructed by carving into the rock of the hill with manual tools and observing the traces left by them on its walls [40]. From the point of view of dating, according to some historians, it was built somewhere between the 11th and 14th centuries [41,42], and others approximate its construction to be much earlier (8th–9th centuries) [40].

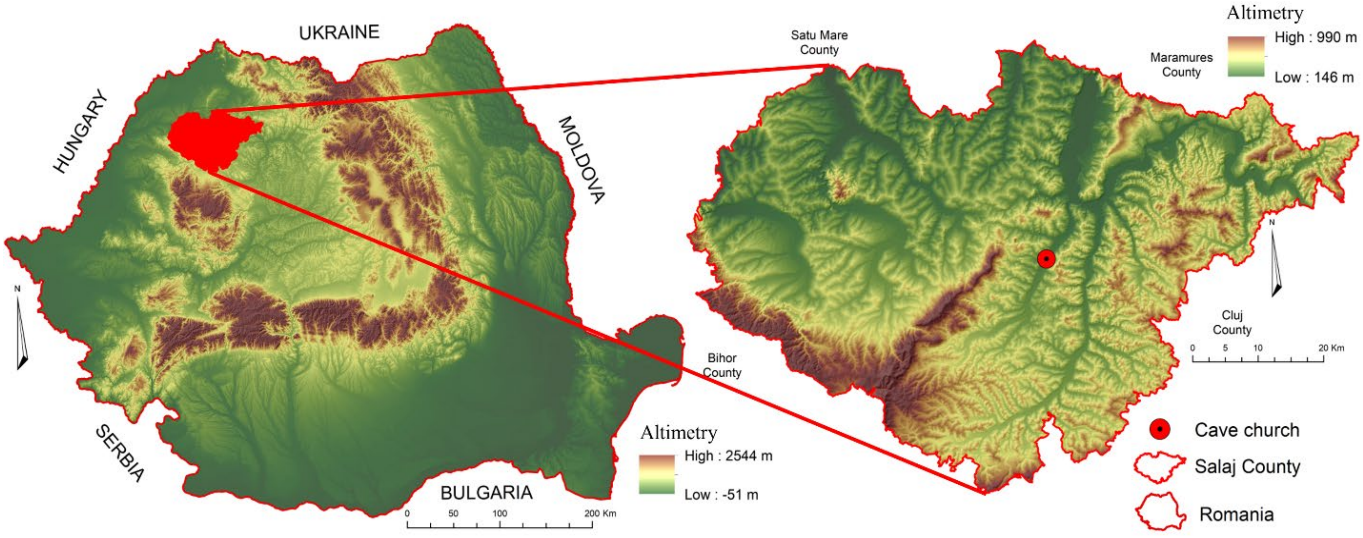

Figure 1. The location of the rupestrian church at the level of Romania and Salaj County.

The monument is divided into two distinct rooms. The entrance is constructed on the north side through a gap in the door, where traces of the old framing can still be seen, wherein the wooden pillars were fixed, which the church door was possibly attached to. The first room, the largest, has a rectangular shape oriented in the north–south direction, two carved niches, and a bench protruding from the vertical line of the wall that can be seen on the south wall of the room, which is probably the dining table altar [41,42].

The analyzed case study was chosen due to its complexity and relevance in the context of the deterioration of natural rocks by microorganisms. This church, located in Sălaj County, Romania, represents a historical monument of national importance, which provides an ideal framework for investigating biodeterioration phenomena due to colonizing microorganisms. It is also essential to rigorously assess the risks to which the monument is exposed in order to implement appropriate preventive measures and ensure the long-term preservation of this element of historical heritage (Figure 2).

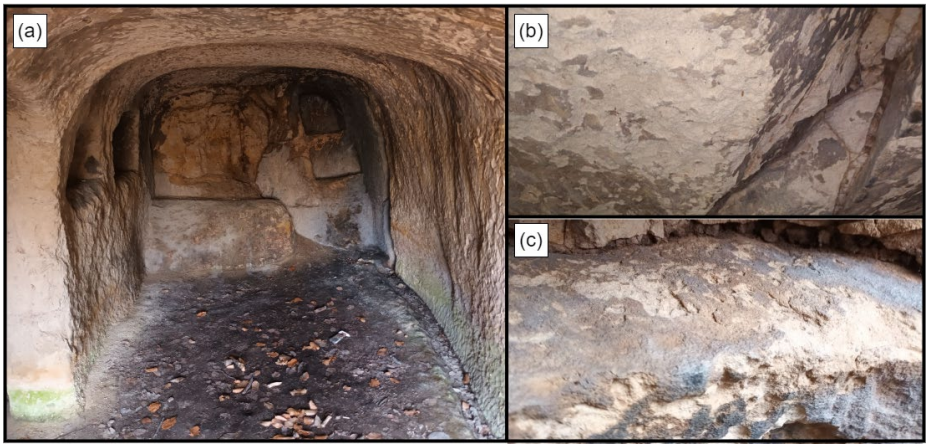

Figure 2. The interior of the rupestrian church. (**a**): The first room of the rupestrian church; (**b**,**c**): damaged areas on the interior walls of the rupestrian church.

For the evaluation of the rupestrian church, three types of analysis were implemented, which involved different ways of taking data and samples, processing them, and interpreting the results (Figure 3). First of all, the collection of rock samples from the walls of the church was considered in order to determine the mineralogical composition of the constituent material. After obtaining this information, the characteristics of the internal and external microclimates were determined in order to determine if they had the potential to cause damage to the material from which the monument is constructed. At the same time, the determination of the external microclimate (in the immediate vicinity of the monument) leaves the possibility of comparing the two environments in order to determine the possible influences. The last stage of the work methodology involved the analysis of fungal and bacteriological contamination of the air and surfaces in order to determine the risks to which the rock is exposed due to the action of microorganisms (Figure 4).

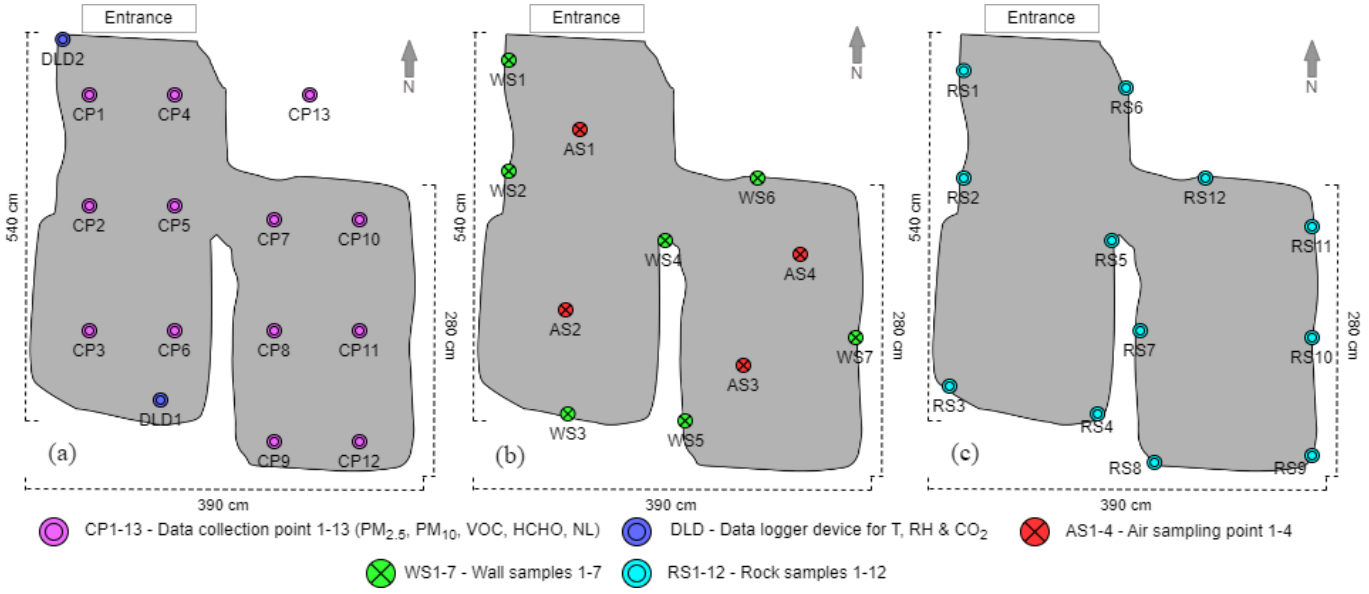

Figure 3. Data collection points, samples, and samples inside the rupestrian church. (**a**) Data collection points regarding the internal microclimate; (**b**) air and surface sample collection points to determine the fungal and bacteriological microflora; (**c**) points of collecting samples for determining the mineralogical composition.

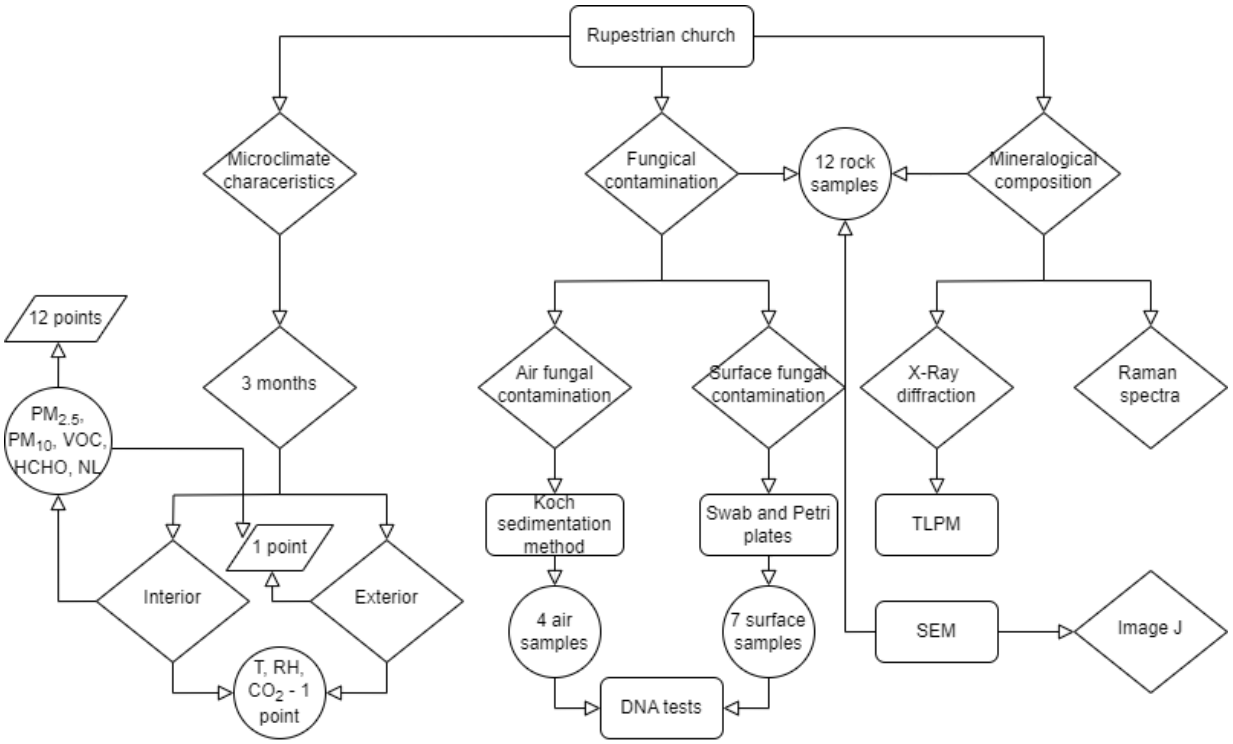

Figure 4. A diagram containing the work steps.

2.1. The Determination of Mineralogical Composition

To determine the mineralogical composition, 12 rock samples were collected from the walls of the rupestrian church. The collection sites were distributed in such a way as to cover the entire interior of the structure (Figure 3c). The process was non-invasive for the monument, considering that only already detached samples were taken; this was important because there was no need to intervene to detach the rock. Furthermore, only the surface part of the detachment was used for the analyses.

XRD and Raman spectra (RS) analyses were performed on the 12 samples to determine the types of minerals. XRD is a valuable method for studying crystalline phases contained in rocks, and the structural analysis of the investigated sample is also corroborated with the other applied experimental methods. The XRD analyses were performed at room temperature using a Rigaku SmartLab multipurpose diffractometer, using Cu Kα_1 radiation (λ = 1.54056Å) equipped with a 9 kW rotating anode. SmartLab Guidance (v.2) software was used to acquire the experimental data. The sample was ground to a fine, homogeneous powder using an agate pestle and mortar and mounted in a sample holder. The measurement was performed in the 5–90° range in steps of 0.01°. Observation on thin sections was conducted using transmitted light polarized microscopy (BX51 Olympus, Tokyo, Japan), equipped with UMPlanFl objective lenses (5×, 10×, and 20×). A circular cross-polarized filter (λ = 137 nm) was used to quantify the texture (i.e., reduction of minerals extinction and intensity of the interference colors).

RS were obtained at room temperature with a Raman Spectrograph Horiba Jobin-Yvon RPA-HE 532 with a multichannel air-cooled (−70 °C) charge-coupled device (CCD) detector, using a Nd-Yag laser 532 nm excitation source and a nominal power of 100 mW. Spectra were obtained in the spectral range between 210 and 3400 cm^{-1} with a spectral resolution of 3 cm^{-1}. The Raman system includes a Superhead fiber optic Raman probe for non-contact measurements with a 50× LWD Olympus objective lens, numerical aperture (NA) = 0.50, working distance (WD) = 10.6 mm, and FIB50/10M optical fiber. The laser spot diameter on the sample surface was approximately 2–3 µm (the minimum theoretical spot diameter is 1.3 µm). Sulfur and cyclohexane were used for the calibration. Data acquisition was performed at a laser power of 1–53.6 mW on the sample's surface. Furthermore, the

laser power was gradually increased by 1% until any photochemical degradation was observed. Spectra manipulations consisted of basic data treatment, such as smoothing adjustments and peak fitting (Lorentz function).

The use of RS to complement XRD offers the advantage of a more comprehensive characterization of samples by identifying both crystalline structures and amorphous phases, to which XRD is less sensitive. RS can detect chemical bonds and organic compounds not visible by XRD, making it useful in the analysis of biodeterioration and organic contaminants. RS also enables non-destructive analysis with minimal sample preparation, providing details of molecular structure and the possibility of mapping compositions on a microscopic scale.

2.2. The Determination of the Microclimate Characteristics

The internal microclimate was determined in both rooms of the church, as well as in its immediate vicinity, in order to correlate the values obtained inside with those outside. Thus, the analyzed indicators were temperature T, RH, the concentration of CO_2, particulate matter ($PM_{2.5}$, PM_{10}), the total amount of volatile organic compounds (VOCs), formaldehyde (HCHO), and natural light (NL). These indicators were analyzed due to the fact that they represent factors with a high destructive potential on natural stone if they are not kept within normal limits.

The data were collected over a period of 12 weeks between April and June 2024. The monitoring was carried out in this period in order to capture the conditions characteristic of spring and early summer, when T and RH fluctuations are significant and favor microbial activity, thus contributing to stone deterioration. This period offers the opportunity to observe the direct impact of variable microclimatic conditions on biodeterioration.

Two different techniques were individualized to determine the indicators. For the determination of $PM_{2.5}$, PM_{10}, VOC, HCHO, and NL, the data were collected manually using 13 individual points (12 inside the church and 1 outside). The values were determined at three different times of the day: in the morning (7), at midday (13), and in the evening (19). The data collection points were positioned in such a way as to obtain the best possible coverage of the rooms, leaving at the same time the possibility of performing some analyses of the distribution of these parameters at the level of the church (Figure 3a). T, RH, and CO_2 were monitored using two data logger sensors, which aimed to record data automatically. All sensors were set to capture data at hourly intervals to obtain as large of a database as possible. One sensor was positioned inside the first room of the church, and the second was positioned at the entrance to the monument (Figure 3a).

T, RH, and CO_2 were determined using two Extech SD800 type datalogger devices (Extech Instruments, Nashua, NH, USA). The accuracy of the device is $\pm$40 ppm for CO_2 concentration measurement, $\pm$0.8 °C for T measurement, and $\pm$4% for RH determination. The data collection was performed at a 1 m distance from the ground, the sampling time being 1 min/point, and the average of all values obtained for that minute being validated.

Total air volume PM concentration was determined using a PCE-PCO 2 portable device (PCE Instruments UK, Southampton, UK). This instrument has the capability to analyze indoor air samples and display the concentration of suspended particles separately for the sizes of 0.3 µm, 0.5 µm, 1.0 µm, 2.5 µm, 5.0 µm, and 10 µm. In the present study, only particles with sizes of 2.5 µm and 10 µm were analyzed. The device determines the indicators with an error of up to 5% and allows the saving of 5000 data sets in the internal memory. The air sampling time to determine the concentration of $PM_{2.5}$ and PM_{10} was 30 sec/collection point.

VOC and HCHO concentrations were determined using a BLATN BR-smart-123s device (BLATN Science and Technology, Beijing, China). It has measuring ranges between 0 and 5.0 mg/m^3 for HCHO and between 0 and 9.9 mg/m^3 for VOCs. The measurement resolution for both indicators was 0.001 mg/m^3, and the margin of error was up to $\pm$5%.

NL was measured three times a day using an Extech SDL400 datalogger lux meter (Extech Instruments, Nashua, NH, USA). This device indicates the amount of light in lux, with an accuracy of ±4%, having the ability to save the recorded values.

ArcGIS 10.8.2, Matlab R2024a, and Microsoft Excel 6.2.14 programs were used to analyze the obtained values.

2.3. The Determination of the Fungal Contamination

The Koch sedimentation method was used to evaluate the fungal contamination of the air. For the Koch method, Sabouraud agar plates consisting of 40 g/L glucose, 10 g/L peptone, 15 g/L agar, and 50 µg/mL chloramphenicol at pH 5.6 were used [43]. Three plates were placed in four distinct points in the investigated cave and left open for 10 min. Swabs were also employed to collect samples from the rupestrian church (Figure 3b). After collection, all samples were sealed using parafilm. All investigations performed on the fungal samples took place in the Molecular Biology Center at the Institute of Interdisciplinary Research on Bio-Nano-Sciences of Babeş-Bolyai University in Cluj-Napoca, Romania, according to standard procedures applied to microbiological sample handling [44]. The plates used for the Koch method were incubated at 20 °C for 10 days. The Omelianski formula (CFU/m^3 air = n*10,000/S*k, where n = number of colonies developed on the plate; S = surface of the Petri dish (∅90 mm); k = air exposure time coefficient: k = 1 for 5 min, k = 2 for 10 min, k = 3 for 15 min, etc.) was used to estimate the fungal colony-forming units (CFUs) present in cave's air.

The swabs were washed in 1 mL of saline solution and 150 µL of the resuspended cells were inoculated on Sabouraud agar plates. For each swab, the inoculations were run in triplicates. The plates were incubated at 20 °C for 10 days.

For every 10-day-old independent colony obtained on plates, the DNA was extracted using the Animal and Fungi DNA Preparation Kit® (Jena Bioscience, Jena, Germany) according to the manufacturer's instructions. The polymerase chain reaction (PCR) amplifications were carried out in a 25 µL final volume consisting of 1× MyTaq Reaction Buffer (Meridian Bioscience®, London, UK), 0.5 mM of each primer (Macrogen Inc., Seoul, South Korea), 1.25 U MyTaq Red DNA Polymerase (Meridian Bioscience®, London, UK), and 50–100 ng of DNA template. The PCR program consisted of the following conditions: initial denaturation at 95 °C for 5 min; 35 cycles of 95 °C for 30 s (denaturation); 56 °C for 30 s (annealing); 72 °C for 30 s (elongation); and final elongation at 72 °C for 5 min. The identification of the isolated fungi was based on the ITS region, and the utilized primers for the PCR amplifications were ITS 1 (5′-TCCGTAGGTGAACCTGCGG-3′) and ITS 4 (5′-TCCTCCGCTTATTGATATGC-3′). The DNA fragments generated by PCR processing were extracted from the agarose gel using the commercial kit NucleoSpin™ Gel and PCR Clean-up (Macherey-Nagel, Ping-Tung, Taiwan) and sequenced using the standard sequencing commercial service at Macrogen (MacrogenEurope, Amsterdam, The Netherlands). Several genera were identified through DNA and metagenomics, including bacteria commonly found in environmental and human-associated habitats. Understanding the specific genera present helps in tailoring conservation strategies to mitigate microbial-induced deterioration [45]. The DNA sequences were submitted to GenBank under the accession numbers PP949376–PP949378.

In addition to the determination of microbiological contamination from the air and from the surfaces inside the rupestrian church, the rock samples were also analyzed with an electronic microscope to highlight the fungi that colonize the rocks and their possible action on the base material. For this, the Phenom ProX scanning electron microscope was used, which is particularly useful in studying different types of materials and their micro- and nano-level structural changes. It allows for the selection of an appropriate magnitude to observe fine surface details and is equipped with an energy-dispersive analysis system, which allows for the identification and quantification of the chemical elements present on the surface of the samples. The SEM analysis was conducted using a high vacuum mode with an acceleration voltage of 30 kV. Both upper and lower secondary electron detectors

were employed to capture detailed images. Two levels of magnification were utilized: a lower magnification for an overall view of the samples and a higher magnification to closely examine the surface topography.

The SEM images thus obtained were processed to determine the degree of fungal coverage of the samples. SEM images were imported into ImageJ software (v. 1.54j), where their processing was based on contrast and shape. To improve the differentiation between fungi and constituent minerals, the image contrast was adjusted using dedicated functions; the optimal values were established empirically to clearly highlight fungi and minerals. Grayscale images were binarized to create a black-and-white image using the optimal contrast threshold. Threshold values were manually adjusted for each image to clarify the separation between fungi and constituent minerals. To remove noise and small particles that are not part of the fungi, the median filter with a radius of 1–2 pixels was used.

The percentage coverage was determined as the ratio of the total area covered by fungi to the total image area. The software automatically calculated this ratio and saved it in the result table generated by ImageJ.

3. Results and Discussion

3.1. The Determination of Mineralogical Composition

The whole-rock thin section and the photomicrographs (Figure 5a–f) show the characteristics of a micaceous sandstone [46–48]. The quartz arenite rock is characterized by a poorly sorted grain distribution, predominantly composed of angular to subrounded grains of quartz (>90%), with clastic flakes of muscovite (5–10%) and up to a 5% composition of feldspars (Figure 5). The matrix, comprising 5–10% of the rock, consists of authigenic clay minerals, suggesting an immature texture of the rock. The muscovite flakes are often distorted and bent between the clastic grains, suggesting compaction (Figure 5b,f).

The quartz arenite samples from the church show elongated muscovite grains within monocrystalline quartz grains (Figure 5e,f), suggesting an initial sedimentary environment with muscovite flakes as detrital grains. During diagenesis, silica-rich fluids precipitated quartz crystals around the detrital muscovite grains, embedding them within the quartz matrix. The elongated shape suggests compaction during burial and diagenesis.

RS analyses have revealed the presence of quartz (SiO_2) and muscovite [$KAl_2(AlSi_3O_{10})(OH)2$] in the sample, confirming the mineral composition observed in the thin sections. The Raman spectrum of the sample has the strong characteristic Raman peak of quartz located at 467 cm^{-1}, which is attributed to the ν_1 symmetric stretching of Si–O–Si [49]. The peaks at 412 cm^{-1} and 1087 cm^{-1} can be assigned to muscovite. Figure 6 shows the recorded Raman spectrum of the sample of the present study compared with the reference RS of quartz (R150091) and muscovite (R150091) from the RRUFF database.

XRD is a suitable method for investigating crystalline phases contained in various rocks. The structural analysis of the investigated sample was also corroborated with the other applied experimental methods.

The powder X-ray pattern is presented in Figure 7 and highlights the presence of four minerals. Silicon oxide found in the form of quartz, SiO_2 (PDF 00-087-2096), is the dominant mineral, highlighted by the intense peak that appears at $2\theta = 26.6^\circ$ and a series of smaller peaks that appear at high diffraction angles.

Another two present phases are muscovite and illite, with the latter acting as a cohesion agent of the muscovite crystals, both being identified by the specific diffraction peak at $2\theta = 8.80^\circ$ and other peaks seen at 17.5° and 26.8°.

Kaolinite represents another constituent phase whose presence is indicated by the slightly broader diffraction peaks compared with the rest of the phases and appears at $2\theta = 12.21^\circ$, 21.0°, and 24.8°.

We can conclude that by using XRD, the quartz and muscovite were both confirmed (Figure 7). Moreover, the clay matrix comprises kaolinite and some illite, both of which were identified only with XRD analysis (Figure 7).

Sandstone, like other sedimentary rocks, is susceptible to biodeterioration due to microbial activity. Over time, depending especially on the climate conditions, fungal colonization and activity can contribute to the degradation of sandstone, resulting in changes in time to its texture, color, and mechanical properties [50].

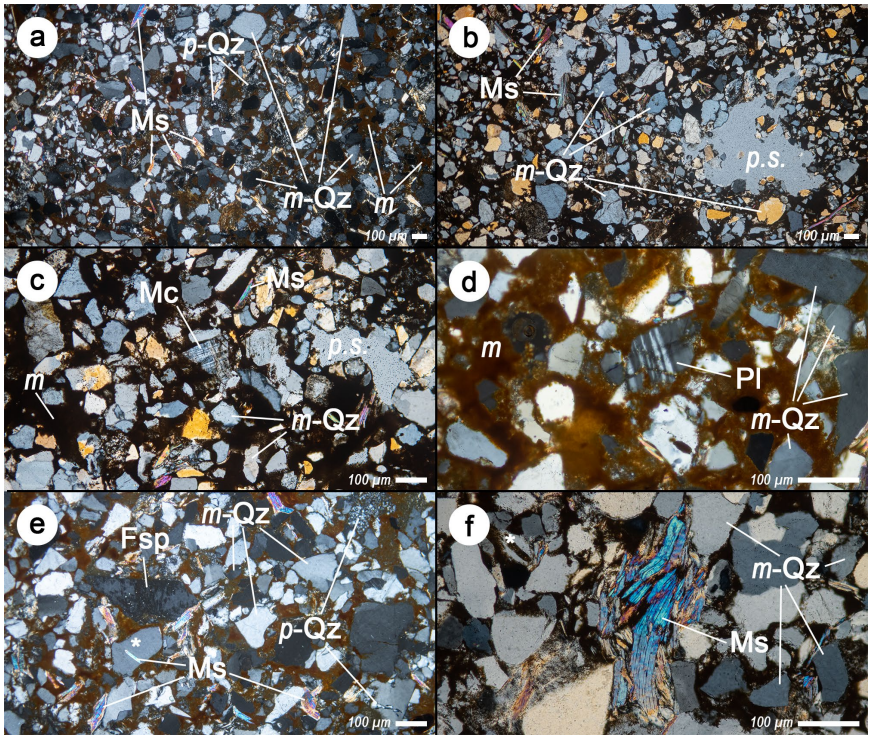

Figure 5. (**a**,**d**,**e**) Photomicrographs of quartz arenite samples under cross-polarizers; (**b**,**c**,**f**) circular cross-polarizers. Abbreviations: m-Qz = monocrystalline quartz; p-Qz = polycrystalline quartz; Ms = muscovite; Pl = plagioclase; Fsp = feldspar; p.s. = pore space; m = clay matrix; * = muscovite crystals embedded in quartz. Scale bars on the photomicrographs are 100 µm.

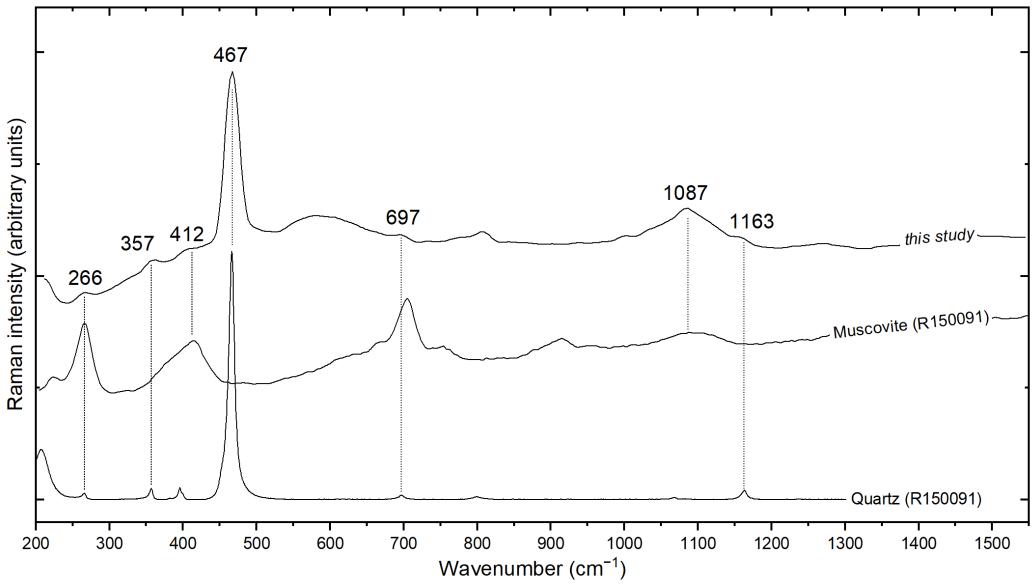

Figure 6. Recorded Raman spectrum of the sample of the present study compared with the reference RS of quartz (R150091) and muscovite (R150091) from the RRUFF database [51].

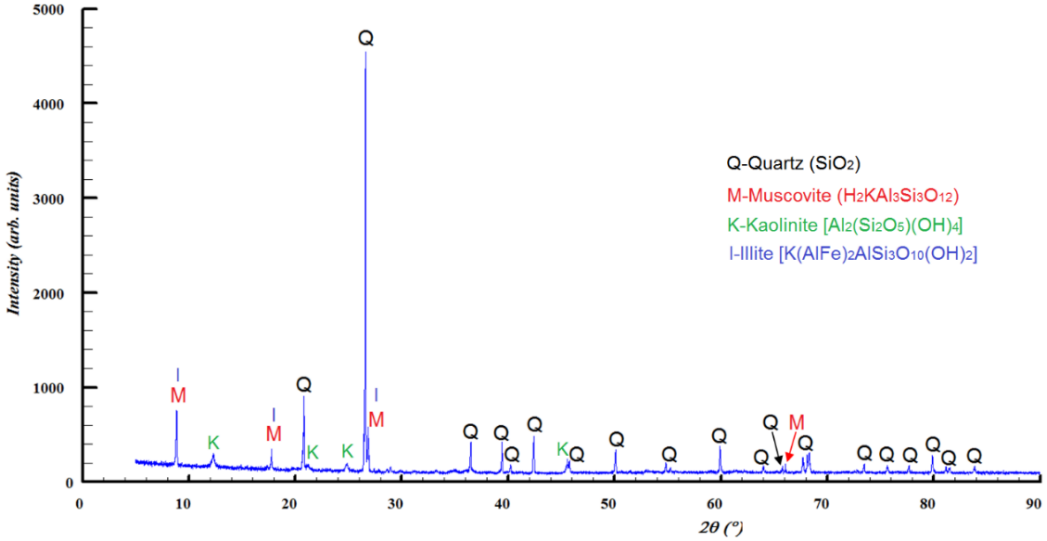

Figure 7. The diffraction pattern shows mineral assemblages of the quartz arenite sample from rupestrian church.

Experimental XRD patterns were recorded at room temperature using a Rigaku SmartLab multipurpose diffractometer, using Cu Kα_1 radiation (λ = 1.54056 Å) and equipped with a 9 kW rotating anode. SmartLab Guidance (v.2) software was used to acquire the experimental data. The sample was ground to obtain a fine homogeneous powder using an agate pestle and mortar and mounted in a sample holder. The measurement was performed in the 5–90° range in steps of 0.01°.

The powder X-ray pattern is presented in Figure 7 and highlights the presence of four minerals. Silicon oxide (found in the form of quartz, SiO_2) is the dominant mineral [52], being highlighted by the intense peak that appears at 2θ = 26.6° and a series of smaller peaks that appear at higher diffraction angles.

Another two present phases are muscovite and illite, which act as cohesion agents of the muscovite crystals. Both are identified by the specific diffraction peak at 2θ = 8.80 [53] and other peaks seen at 17.5° and 26.8°.

Kaolinite ($Al_2(Si_2O_5)(OH)_4$) represents another constituent phase [54] whose presence is given by the slightly broader diffraction peaks compared with the rest of the phases and appears at 12.21°, 21.0°, and 24.8°.

3.2. The Determination of the Microclimate Characteristics

In order to protect the artifacts of the cultural and natural heritage, the internal microclimate must be kept as much as possible within the accepted limits, avoiding large and frequent fluctuations. Regarding objects created from stone, they fall into a broader category of artifacts, which are individualized by the need to regulate the internal microclimate between 15 and 25 °C in terms of T, with fluctuations of a maximum of ±4 °C during 24 h [55]. Lower Ts are preferable to slow chemical reactions that can damage materials. For RH, a range of 40–60% is recommended, with a maximum fluctuation of ±5% during 24 h. Stable RH values are crucial to prevent damage through the expansion and contraction of materials [56]. Regarding the present study, T varies within a gap of 20.6 °C, ranging from a minimum of 3.9 °C to a maximum of 24.5 °C; the average over the entire monitoring period is 9.8 °C. As far as the average is concerned, it falls within the standards; however, the hourly values fluctuate quite a lot and frequently. At the same time, in 99.5% of cases, the T values are below the minimum allowed value of 15 °C (Figure 8). Given that the study concerns a rupestrian church, the T values are expected to fluctuate frequently and often be below the permissible minimum of 15 °C. This behavior is mostly normal for the specific cave environment, where microclimatic conditions are influenced by natural factors such as heat transfer and natural cave ventilation [57]. The RH values obtained inside the

church indicate an average of 90.6%, with maximums of 99.7% and minimums of 43.6%; the difference in which the values varied was 56.1%. At the same time, in 99.5% of the cases, the RH values exceeded the upper limit of acceptability, which can affect the integrity of the minerals in the rocks (Figure 8). In the presence of high RH, soluble salts can be transported to the surface of the rocks and, as the water evaporates, they crystallize. The crystallization of salts can generate high internal pressures that can lead to the cracking and disintegration of rocks. In addition, high RH levels favor the development of microorganisms, including molds and bacteria, which can produce organic acids capable of dissolving minerals [58]. A high RH can accelerate chemical reactions that lead to mineral alteration. For example, oxidation-reduction reactions and hydrolysis can be enhanced under high RH conditions, which can damage the mineral structure [18].

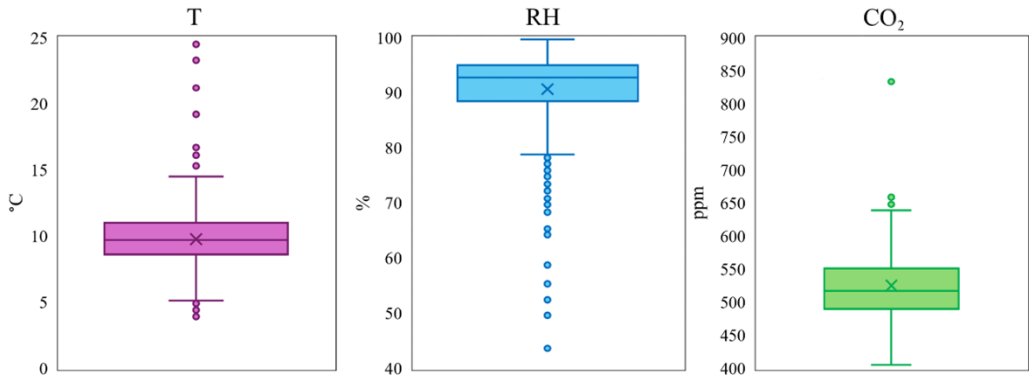

Figure 8. The values obtained for the T, RH, and CO_2 indicators during the period of April–June 2024 inside the rupestrian church.

Although there are no specific standards for CO_2 levels in caves alone, it is essential to keep concentrations as close as possible to natural atmospheric levels (~400–500 ppm) to prevent the formation of carbonic acid, which can accelerate mineral degradation [57,58]. Most of the time, the CO_2 values remain within normal limits, with some peaks exceeding 600 ppm, the maximum reaching 834 ppm. However, the variations are insignificant, and the high values are only sporadic. The average value indicates 525 ppm, and the minimums reach 405 ppm on multiple occasions. Approximately 88% of the measured data are below the limit of 600 ppm (Figure 8). Considering the fact that there is no human activity inside, these small variations in the amount of CO_2 can be determined by the respiration of organisms (small animals, microorganisms, or plants), soil and rock interactions (decomposition of organic matter), or the air exchange between the cave and the outside environment [59,60]

CO_2 variability can influence the chemical balance in the cave, affecting the formation and stability of speleothems and other mineral structures. In the long term, even minor fluctuations can cause changes in rocks' chemical composition, especially through carbonic acid formation [60]. Thus, although high values are sporadic, the cumulative effects of periodic increases in CO_2 can contribute to the progressive degradation of minerals, especially in the presence of constant high levels of RH, which facilitate chemical reactions [61].

Fine and coarse particles ($PM_{2.5}$, PM_{10}) can act as abrasive agents, leading to the erosion of mineral surfaces and deposition of chemicals that can react with rocks [62]. VOCs and HCHO can lead to chemical reactions that form organic acids, accelerate the alteration of minerals, and cause the growth of microorganisms that contribute to biodegradation [63]. At the same time, the photooxidation process is activated by natural light and involves chemical reactions that break down organic and inorganic matter. This can lead to rock surface chemical and physical modification, making them brittle and more susceptible to erosion [64]. International standards regulate the concentrations of $PM_{2.5}$, PM_{10}, VOCs, and HCHO to protect human health, such as those established by the World Health Organization. However, specific standards for protecting rock integrity are less common,

and general recommendations include keeping concentrations of these pollutants as low as possible. In the case of NL, international standards indicate that for less sensitive objects, such as metal, ceramics, stones and glass, they can be continuously exposed to an illumination of up to 300 lux without affecting their integrity [65].

$PM_{2.5}$ recorded an average value inside the church of 4.2 μg/m^3; in its immediate vicinity, the values were 6.4 μg/m^3. The maximum values reached 8 μg/m^3 indoors and 12 μg/m^3 outdoors, with the minimum being 0 μg/m^3 indoors and 2 μg/m^3 outdoors. Regarding the spatial distribution of $PM_{2.5}$ within the church, the highest average values over the entire monitoring period are identified at the entrance to the church (between 5.2 and 5.8 μg/m^3) and in the first room within it, because in the second room, the values reach a maximum of 4.3 μg/m^3 and a minimum of 3 μg/m^3 (Figure 9). In the case of PM_{10}, the average values were 8.9 μg/m^3 indoors and 12.8 μg/m^3 outdoors, with maximum values of 15 μg/m^3 and 24 μg/m^3 and minimum values of 1 μg/m^3 and 4 μg/m^3, respectively. The spatial distribution of this indicator follows the evolution of coarser particles ($PM_{2.5}$), with averages ranging between 10.1 μg/m^3 and 10.5 μg/m^3 at the entrance to the church, and a downward evolution of the concentration up to the second room, where the maximum was 8.7 μg/m^3, and the minimum was 7 μg/m^3 (Figure 9).

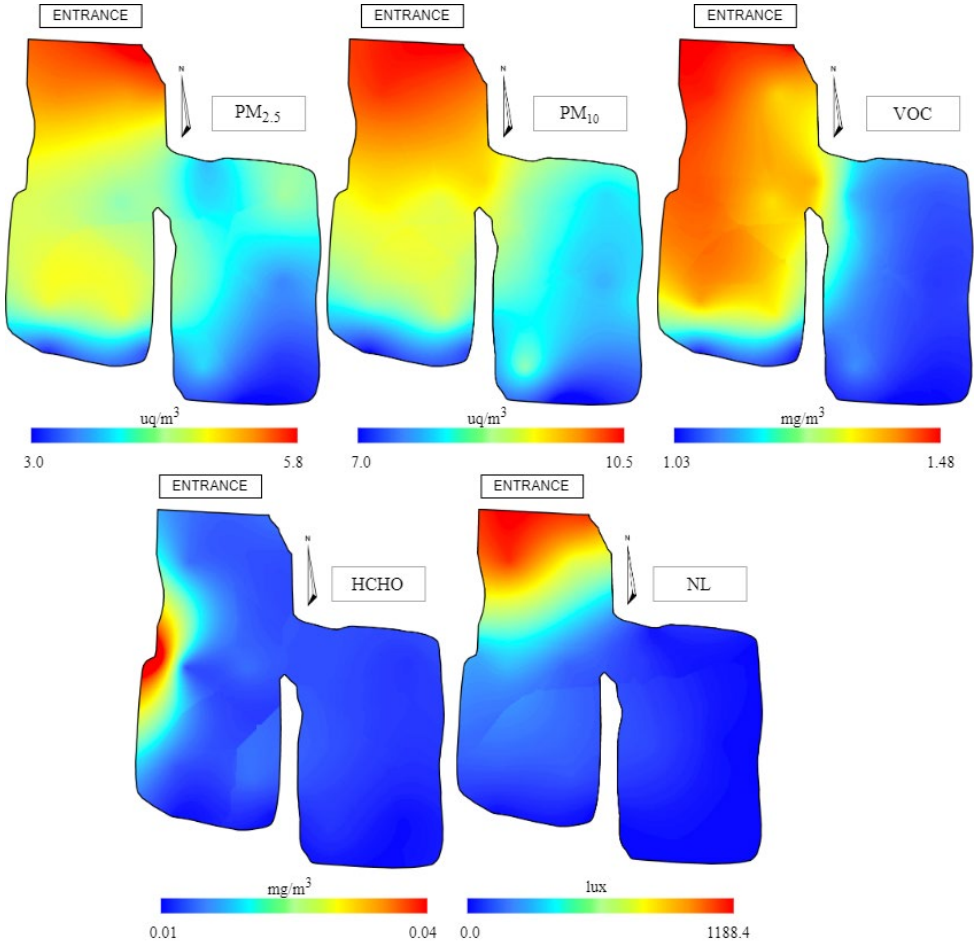

Figure 9. The spatial distribution at the church level of the average values of $PM_{2.5}$, PM_{10}, HCHO, VOCs, and NL (the values represent the average for each collection point).

Regarding the co-concentration of VOCs, the indoor average during the analyzed period was 1.24 mg/m^3, with a minimum of 0.33 mg/m^3 and a maximum of 3.78 mg/m^3. The exterior showed an average value of 1.62 mg/m^3, with a minimum of 0.78 mg/m^3 and a maximum of 4.11 mg/m^3. The spatial distribution indicates higher values at the entrance to the monument (up to 1.48 mg/m^3), which gradually decrease in the first and second

rooms, up to minimum values of 1.03 mg/m^3 (Figure 9). This indicates a close connection between the exterior and interior, with interior values being largely influenced by the VOC concentration in the exterior environment. The HCHO values also fluctuate in the same pattern, registering higher values in the first room (up to 0.04 mg/m^3), decreasing and reaching a minimum of 0.01 mg/m^3 in the second room and the lower part of the first one. The average of this indicator was 0.02 mg/m^3 indoors and 0.03 mg/m^3 outdoors (Figure 9).

The average quantity of NL was in line with the international standards in terms of intensity, reaching 247.4 lux. The minimum was 0 lux and the maximum 1188.4 lux, but in 92.3% of cases, the values did not exceed 300 lux. The spatial distribution indicated, as in the case of the other indicators, very high values at the entrance to the monument (over 1000 lux in three points and over 600 lux in two points) and low values inside (under 200 lux in the first room and under 70 lux in the second), indicating the close relationship between exterior and interior) (Figure 9).

In addition to the destructive effects that the action of these pollutants can have on the minerals in the base rock, they also play a vital role in the development of fungi. Thus, fungi are highly influenced, especially by T and RH; they develop best in conditions of T below 10 °C and RH above 85%, with species such as *Fusarium* and *Cephalosporium* thriving in these levels [66,67]. The respective microclimate conditions are also found in the current case study. *Aspergillus* and *Penicillium* species showed varied responses to CO_2 concentrations. Some species can grow at high CO_2 levels (up to 60%) but show reduced growth and mycotoxin production under such conditions [68]. These species of fungi are also associated with $PM_{2.5}$ and PM_{10}, which are significant components that contribute to the production of organic carbon and the mass of aerosols in the atmosphere [69]. As for HCHO and VOCs, these indicators can also facilitate additional microbial growth and affect the integrity of materials and artifacts, especially VOCs like 3-methyl-1-butanol and 1-octen-3-ol [70].

3.3. The Determination of the Fungal Contamination

The fungal loads and the degree of contamination of the air samples were estimated based on indoor applied standards (Table 1) [71]. The Petri dishes used for the Koch method can be observed in Figure 10.

Table 1. Fungal loads in the air in the rupestrian church.

Air Sample	Number of Fungal CFU/m^3 of Air	Degree of Contamination
AS1	892	High
AS2	580	High
AS3	367	Medium
AS4	1102	High

Porca et al. [72] proposed standards that characterize the cave's atmosphere based on the identified fungal loads in the air samples. Point AS3 falls into category III (between 150 and 500 CFU m^{-3})—threatened by fungi and requires different cave management and controls—while AS1 and AS2 fall into category IV (between 500 and 1000 CFU m^{-3})—already affected by fungi as a result of massive visits or spillage—and AS4 falls into category V (above 1000 CFU m^{-3})—having irreversible ecological disturbance.

Cladosporium herbarum (belonging to the genus *Cladosporium*, phylum *Ascomycota*), *Aspergillus niger* (belonging to the genus *Aspergillus*, phylum Ascomycota), and *Mortierella hyalina* (belonging to the genus *Mortierella*, phylum *Mucoromycota*) are the fungal species identified in the analyzed isolates. Their abundance varies in the different collection points (Figure 11). *Cladosporium herbarum* is present in all analyzed collection points, while *Aspergillus niger* is absent in one wall sample (WS1) and *Mortierella hyalina* in three wall samples (WS3, WS4, and WS5).

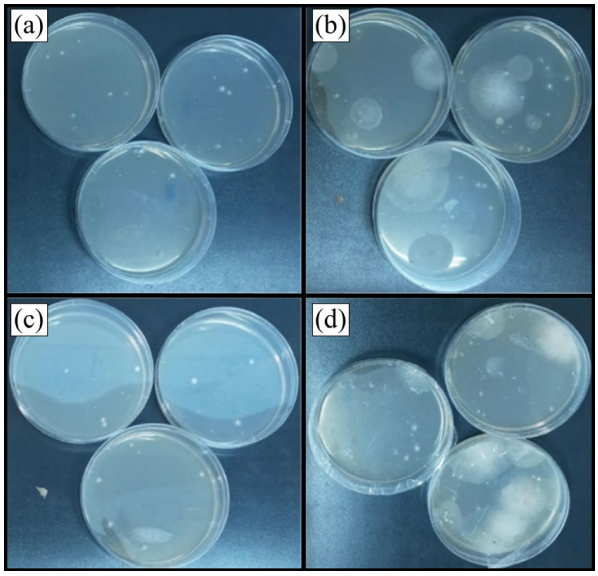

Figure 10. Petri dishes were used for the fungal load estimation in the associated air by the Koch method for the collection sample points 1 (**a**), 2 (**b**), 3 (**c**), and 4 (**d**).

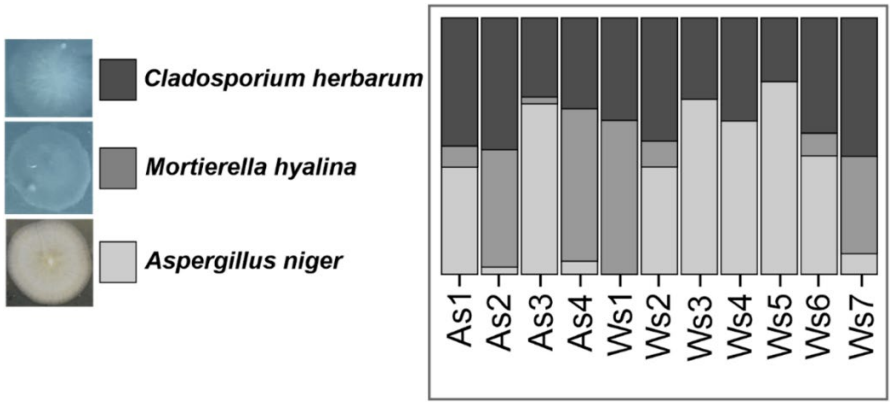

Figure 11. Identified fungal species in the analyzed rupestrian church in the samples collected from the air and walls and abundance plots of the fungal isolated from each collection point.

All the identified species are frequently reported as cave inhabitants [73–76]. *Cladosporium herbarum* is frequently present in the air and wall samples in caves worldwide [73,77]. *Cladosporium herbarum* is present in the inside air as well as in the outside air. Usually, its frequency is much higher outside, a fact that makes it one of the most frequent contaminants. *Aspergilus niger* can be also present in air and wall samples [73,77]. In contrast to *Cladosporium herbarum*, *Aspergilus niger* is more frequent in the inside air than the outside [73]. *Mortierella* species are cosmopolitan fungi frequently recovered from soils where they maintain a saprotrophic lifestyle. They can also be plant pathogens. The species are commonly found in subterranean environments and show metal tolerance. *Mortierella hyalina* is a root-colonizing fungi, and its presence may be associated with the agricultural fields near the rupestrian church entry.

SEM images processed with ImageJ software (Figure 12) reveal the presence of fungal hyphae and spores on and within the matrix of the kaolinite–illite mineral assemblage. This can be attributed to various bio-geological processes (i.e., sedimentary deposition, diagenesis, and mineral alteration). Fungal hyphae can infiltrate sediments, releasing nutrients and forming fungal networks. In environments with clay minerals, fungal activity can contribute to the breakdown of organic matter and the alteration of clay minerals.

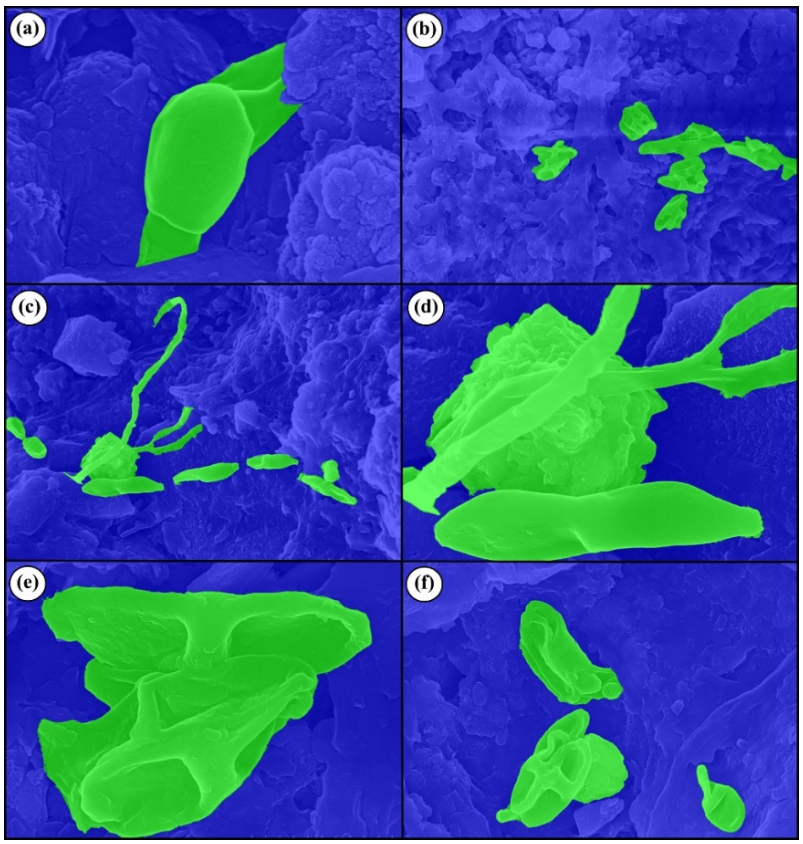

Figure 12. Processed SEM images of the samples of sandstone from the rupestrian church. The green color suggests the presence of identified fungal hyphae and spores on and within the matrix of the kaolinite–illite assemblage (blue) (**a**–**f**)—different SEM images of the analyzed samples).

Aspergillus and *Cladosporium* have been reported as biodeteriogens on objects, monuments, etc., belonging to the cultural patrimony with a natural stone support. Their identification and evaluation of biodeterioration, often materialized by discoloration, pigmented patina, powdering, and dissolution [78,79], precede restoration and conservation activities. The mentioned fungi can produce enzymes, pigments, and organic acids such as gluconic, succinic-malic, oxalic, and citric acid with the release of calcium by the rock it colonizes, and it has the possibility of developing calcium oxalate microcrystals, which irreversibly damage the artifacts with calcareous support [27,80–82]. *Cladosporium hyphae* can penetrate the rock, leading to structural changes (and acting through biopitting) due to various acid metabolites (organic or siderophores) that dissolve component minerals of the stone using biomineralization and secondary mycogenic actions with the development of the colony and penetration into the depth of the rock [18,27,28,83,84]. Chemoorganotrophic fungi such as *Aspergillus* damage the stone. However, by infiltrating the hyphae, they manage to penetrate inside and exert a biocorrosive activity (due to excreted organic acids, the oxidation of cations generating neominerals, etc.) and contribute to the discoloration of stone surfaces, and the excretion of melanin leads to the installation of colored patina [85–87] and mechanical stress. Polymeric substances applied to the stone with a protective role can be attacked by *Aspergillus* colonies [88–90].

4. Conclusions

This study has provided a comprehensive analysis of the factors contributing to the deterioration of natural stone in the rupestrian church in Jac, Romania, focusing on the combined effects of microclimatic conditions and microbial activity. The findings underscore the multifaceted nature of stone degradation, influenced by physical, chemical, and biological processes. The physical disaggregation of stone is significantly influenced by

environmental conditions such as T fluctuations and RH variations. The freeze–thaw cycles, common in the Romanian climate, cause expansion and contraction within the stone's pore structure, leading to mechanical stress and eventual cracking. The data collected over 12 weeks demonstrated substantial T and RH variations within the church, contributing to this type of weathering. Chemical weathering is another critical factor affecting the integrity of the stone. The solubilization of minerals by organic and inorganic acids, as observed in the sandstone samples, plays a significant role in the chemical breakdown of the stone. RS and XRD analyses confirmed the presence of quartz, muscovite, and feldspars, which are susceptible to dissolution under acidic conditions. The high levels of VOCs detected within the church further exacerbate this chemical weathering process. Through oxidation and other chemical reactions, VOCs can produce acids that accelerate the deterioration of the stone's mineral composition. The biological aspect of stone deterioration was a central focus of this study. The culture-based identification methods revealed the presence of several fungi, including *Cladosporium herbarum*, *Aspergillus niger*, and *Mortierella hyalina*. These fungi contribute to biodeterioration through biocorrosion and biomineralization processes. SEM images provided visual evidence of fungal hyphae and spores infiltrating the kaolinite–illite matrix, demonstrating the extent of microbial colonization. The metabolic activities of these microorganisms lead to the production of organic acids and enzymes that further degrade the stone's structure. This study also identified that high church RH levels create an ideal microbial growth environment. With RH averaging 90.6% and often exceeding 99%, the conditions are highly conducive to fungal proliferation. This excessive moisture supports microbial activity and facilitates the dissolution and transport of salts within the stone, leading to efflorescence and further structural weakening. The comprehensive microclimatic data highlight the interplay between environmental conditions and stone decay. High levels of $PM_{2.5}$ and PM_{10} were observed, which not only have abrasive effects on the stone surfaces but also act as carriers for microbial spores, thus enhancing biological contamination.

Given the multifaceted nature of stone deterioration identified in this study, it is clear that effective preservation strategies must be equally comprehensive. Stabilizing the microclimate within the church is paramount. Additionally, monitoring and reducing indoor pollutants, particularly VOCs and PM, are crucial to preserving the stone's integrity. Biocontrol measures are also essential to mitigate the impact of microbial colonization. Regular cleaning and applying biocides can help control the growth of biodeteriogenic fungi. Furthermore, protective coatings that are permeable to water vapor but resistant to microbial penetration could be applied to the stone surfaces to provide an additional layer of defense (different nanoparticles, siloxane-based coatings, acrylic polymer coatings, silicate-based coatings, alkylalkoxysilanes, etc.).

Author Contributions: Conceptualization, D.C.I. and A.-I.A.; methodology, A.-I.A., C.M., T.C. and L.B.-T.; software, T.H.H. and I.-C.N.; validation, A.I. and B.Z.; formal analysis, N.H. and A.T.; investigation, A.C.P. and I.-C.N.; resources, D.C.I.; data curation, B.S.; writing—original draft preparation, D.C.I., C.M., A.I., T.C., A.-I.A. and A.C.P.; writing—review and editing, B.Z., N.H. and T.H.H.; visualization, B.S.; supervision, D.C.I. All authors have read and agreed to the published version of the manuscript.

Funding: This work was partially supported by the Deanship of Scientific Research, Vice Presidency for Graduate Studies and Scientific Research, King Faisal University, Saudi Arabia [Grant No. KFU241712].

Institutional Review Board Statement: Not applicable.

Informed Consent Statement: Not applicable.

Data Availability Statement: The raw data supporting the conclusions of this article will be made available by the authors without undue reservation.

Acknowledgments: The research undertaken was made possible by the equal scientific involvement of all the authors concerned. This research has been funded by the University of Oradea, Romania.

Conflicts of Interest: The authors declare no conflicts of interest.

References

1. Gupta, S.P.; Kurmi, M.K. Impact of fungi on historical monument with reference to Mahadev temple Bastar of Chhatisgarh. *Int. J. Life Sci. Res. Arch.* **2023**, *4*, 1–5. [CrossRef]
2. Ilieș, D.C.; Blaga, L.; Hassan, T.H.; Ilieș, A.; Caciora, T.; Grama, V.; Herman, G.V.; Dejeu, P.; Zdringa, M.; Marshall, T.; et al. Indoor Microclimate and Microbiological Risks in Heritage Buildings: A Case Study of the Neologic Sinagogue, Oradea, Romania. *Buildings* **2023**, *13*, 2277. [CrossRef]
3. Ilies, D.C.; Blaga, L.; Ilies, A.; Pereș, A.C.; Caciora, T.; Hassan, T.H.; Hodor, N.; Turza, A.; Taghiyari, H.R.; Barbu-Tudoran, L.; et al. Green Biocidal Nanotechnology Use for Urban Stone-Built Heritage—Case Study from Oradea, Romania. *Minerals* **2023**, *13*, 1170. [CrossRef]
4. Lajçi, D.; Kuqi, B.; Fetahaj, A.; Osmanollaj, S. The values of cultural heritage in the Rugova Region in promoting the development of tourism in Kosovo. *GeoJ. Tour. Geosites* **2022**, *41*, 502–508. [CrossRef]
5. Pyzik, A.; Ciuchcinski, K.; Dziurzynski, M.; Dziewit, L. The Bad and the Good—Microorganisms in Cultural Heritage Environments—An Update on Biodeterioration and Biotreatment Approaches. *Materials* **2021**, *14*, 177. [CrossRef]
6. Chen, X.; Bai, F.; Huang, J.; Lu, Y.; Wu, Y.; Yu, J.; Bai, S. The Organisms on Rock Cultural Heritages: Growth and Weathering. *Geoheritage* **2021**, *13*, 56. [CrossRef]
7. Bungau, C.C.; Bendea, C.; Bungau, T.; Radu, A.-F.; Prada, M.F.; Hanga-Farcas, I.F.; Vesa, C.M. The Relationship between the Parameters That Characterize a Built Living Space and the Health Status of Its Inhabitants. *Sustain. Sci. Pract. Policy* **2024**, *16*, 1771. [CrossRef]
8. Mabrouk, N.; Rashad, Y.; Elmitwalli, H.; Shabana, Y.; Sreenivasaprasad, P.; Elsayed, Y. Assessment of Some Green Fungicides against Fungi Isolated from Different Heritage Sites and Museums in Egypt. *Sci. Cult.* **2023**, *9*, 101–112.
9. Elsayed, Y.; El-Kadi, S.; El-Rian, M.; Mabrouk, N. The Efficiency of Microbial Culture Extracts as Green Antimicrobial Products against Some Microorganisms Colonizing the Historic Oil Paintings. *Sci. Cult.* **2023**, *9*, 127–143.
10. Scheerer, S.; Ortega-Morales, O.; Gaylarde, C. Chapter 5 Microbial Deterioration of Stone Monuments—An Updated Overview. In *Advances in Applied Microbiology*; Academic Press: Cambridge, MA, USA, 2009; Volume 66, pp. 97–139.
11. Sterflinger, K. Fungi: Their role in deterioration of cultural heritage. *Fungal Biol. Rev.* **2010**, *24*, 47–55. [CrossRef]
12. Suihko, M.-L.; Alakomi, H.-L.; Gorbushina, A.; Fortune, I.; Marquardt, J.; Saarela, M. Characterization of Aerobic Bacterial and Fungal Microbiota on Surfaces of Historic Scottish Monuments. *Syst. Appl. Microbiol.* **2007**, *30*, 494–508. [CrossRef] [PubMed]
13. Gadd, G.M.; Raven, J.A. Geomicrobiology of Eukaryotic Microorganisms. *Geomicrobiol. J.* **2010**, *27*, 491–519. [CrossRef]
14. Suchý, V.; Borecká, L.; Pachnerová Brabcová, K.; Havelcová, M.; Svetlik, I.; Machovič, V.; Lapčák, L.; Ovšonková, Z.A. Microbial Signatures from Speleothems: A Petrographic and Scanning Electron Microscopy Study of Coralloids from the Koněprusy Caves (the Bohemian Karst, Czech Republic). *Sedimentology* **2021**, *68*, 1198–1226. [CrossRef]
15. Wang, Y.; Zhang, H.; Liu, X.; Liu, X.; Song, W. Fungal Communities in the Biofilms Colonizing the Basalt Sculptures of the Leizhou Stone Dogs and Assessment of a Conservation Measure. *Herit. Sci.* **2021**, *9*, 36. [CrossRef]
16. Lazo, D.E.; Dyer, L.G.; Alorro, R.D. Silicate, Phosphate and Carbonate Mineral Dissolution Behaviour in the Presence of Organic Acids: A Review. *Miner. Eng.* **2017**, *100*, 115–123. [CrossRef]
17. Gerrits, R.; Pokharel, R.; Breitenbach, R.; Radnik, J.; Feldmann, I.; Schuessler, J.A.; von Blanckenburg, F.; Gorbushina, A.A.; Schott, J. How the rock-inhabiting fungus K. petricola A95 enhances olivine dissolution through attachment. *Geochim Cosmochim Acta* **2020**, *282*, 76–97. [CrossRef]
18. Gadd, G.M.; Fomina, M.; Pinzari, F. Fungal Biodeterioration and Preservation of Cultural Heritage, Artwork, and Historical Artifacts: Extremophily and Adaptation. *Microbiol. Mol. Biol. Rev.* **2024**, *88*, e0020022. [CrossRef]
19. Domínguez-Villar, D.; Lojen, S.; Krklec, K.; Baker, A.; Fairchild, I.J. Is Global Warming Affecting Cave Temperatures? Experimental and Model Data from a Paradigmatic Case Study. *Clim. Dyn.* **2015**, *45*, 569–581. [CrossRef]
20. Del Mondo, A.; Hay Mele, B.; Petraretti, M.; Zarrelli, A.; Pollio, A.; De Natale, A. Alternaria Tenuissima, a Biodeteriogenic Filamentous Fungus from Ancient Oplontis Ruins, Rapidly Penetrates Tuff Stone in an In Vitro Colonization Test. *Int. Biodeterior. Biodegrad.* **2022**, *173*, 105451. [CrossRef]
21. Saleh, I.; Hady, M.A.; Moussa, A.; Hefni, Y.; El-Latif, M.L.A. Experimental study for the consolidation and protection of sandstone petroglyphs at Sarabit el Khader (Sinai, Egypt). *Sci. Cult.* **2018**, *5*, 43–48.
22. El-Badry, A.E.-H.A.; Ali, F.A.; Ismail, B.M. Assessment of the aging treatments of sandstone greywacke rock art (wadi hammamat) by petrography, SEM, XRD, EDX. *Sci. Cult.* **2023**, *5*, 37–48.
23. El-Sayed, S.S.M.; Maky, A.R.Y. Archaeometric Investigation to Evaluate Acrylic, Silicon Materials and Nano-Additives as Consolidation Material to Sandstone Monuments of the Sphinxes Avenue (Luxor, Egypt). *Sci. Cult.* **2021**, *8*, 51–62.
24. McNamara, C.; Mitchell, R. Microbial deterioration of historic stone. *Front. Ecol. Env.* **2005**, *3*, 445–451. [CrossRef]
25. Moncmanová, A. *Environmental Deterioration of Materials*; WIT Press: Southampton, UK, 2007; ISBN 9781845640323.
26. Sterflinger, K.; Piñar, G. Microbial Deterioration of Cultural Heritage and Works of Art—Tilting at Windmills? *Appl. Microbiol. Biotechnol.* **2013**, *97*, 9637–9646. [CrossRef] [PubMed]
27. Li, T.; Hu, Y.; Zhang, B.; Yang, X. Role of Fungi in the Formation of Patinas on Feilaifeng Limestone, China. *Microb. Ecol.* **2018**, *76*, 352–361. [CrossRef] [PubMed]

28. Ma, Y.; Zhang, H.; Du, Y.; Tian, T.; Xiang, T.; Liu, X.; Wu, F.; An, L.; Wang, W.; Gu, J.-D.; et al. The Community Distribution of Bacteria and Fungi on Ancient Wall Paintings of the Mogao Grottoes. *Sci. Rep.* **2015**, *5*, 7752. [CrossRef]
29. Nugari, M.P.; Pietrini, A.M.; Caneva, G.; Imperi, F.; Visca, P. Biodeterioration of Mural Paintings in a Rocky Habitat: The Crypt of the Original Sin (Matera, Italy). *Int. Biodeterior. Biodegrad.* **2009**, *63*, 705–711. [CrossRef]
30. Favero-Longo, S.E.; Gazzano, C.; Girlanda, M.; Castelli, D.; Tretiach, M.; Baiocchi, C.; Piervittori, R. Physical and chemical deterioration of silicate and carbonate rocks by meristematic microcolonial fungi and endolithic lichens (Chaetothyriomycetidae). *Geomicrobiol J.* **2011**, *28*, 732–744. [CrossRef]
31. Tonon, C.; Breitenbach, R.; Voigt, O.; Turci, F.; Gorbushina, A.A.; Favero-Longo, S.E. Hyphal Morphology and Substrate Porosity-rather than Melanization-Drive Penetration of Black Fungi into Carbonate Substrates. *J. Cult. Herit.* **2021**, *48*, 244–253. [CrossRef]
32. Kim, J.S.; Cho, Y.; Seo, C.W.; Park, K.H.; Yoo, S.; Lee, J.W.; Kim, S.H.; Lee, W.; Lim, Y.W. Fungal Catastrophe of a Specimen Room: Just One Week Is Enough to Eradicate Traces of Thousands of Animals. *J. Microbiol.* **2023**, *61*, 189–197. [CrossRef]
33. Omebeyinje, M.H.; Adeluyi, A.; Mitra, C.; Chakraborty, P.; Gandee, G.M.; Patel, N.; Verghese, B.; Farrance, C.E.; Hull, M.; Basu, P.; et al. Increased Prevalence of Indoor Aspergillus and Penicillium Species Is Associated with Indoor Flooding and Coastal Proximity: A Case Study of 28 Moldy Buildings. *Environ. Sci. Process. Impacts* **2021**, *23*, 1681–1687. [CrossRef] [PubMed]
34. Salvadori, O.; Municchia, A.C. The role of fungi and lichens in the biodeterioration of stone monuments. *Open Conf Proceed J.* **2016**, *7*, 39–54. [CrossRef]
35. Seaward, M.R.D.; Edwards, H.G.M. Biological Origin of Major Chemical Disturbances on Ecclesiastical Architecture Studied by Fourier Transform Raman Spectroscopy. *J. Raman Spectrosc.* **1997**, *28*, 691–696. [CrossRef]
36. Lisci, M.; Monte, M.; Pacini, E. Lichens and Higher Plants on Stone: A Review. *Int. Biodeterior. Biodegrad.* **2003**, *51*, 1–17. [CrossRef]
37. Keshari, N.; Das, S.K.; Adhikary, S.P. Microbial Deterioration of Heritage Monuments in Santiniketan, West Bengal, India. *Curr. Sci.* **2019**, *116*, 709–711.
38. Mang, S.M.; Scrano, L.; Camele, I. Preliminary Studies on Fungal Contamination of Two Rupestrian Churches from Matera (Southern Italy). *Sustainability* **2020**, *12*, 6988. [CrossRef]
39. Cardellicchio, F.; Bufo, S.A.; Mang, S.M.; Camele, I.; Salvi, A.M.; Scrano, L. The Bio-Patina on a Hypogeum Wall of the Matera-Sassi Rupestrian Church 'San Pietro Barisano' before and after Treatment with Glycoalkaloids. *Molecules* **2022**, *28*, 330. [CrossRef]
40. Creaca Town Hall. Pemnita Monului Cave Church. 2017. Available online: https://comunacreaca.ro/biserica-rupestra-pemnita-monului/ (accessed on 21 July 2024).
41. List of Historical Monuments 2015, Salaj County. Available online: https://www.cultura.ro/sites/default/files/inline-files/LMI-SJ.pdf (accessed on 21 July 2024).
42. National Archaeological Inventory (RAN). Information about the Site, the Cave Church from Jac—Pemnita Monului. Available online: https://ran.cimec.ro/sel.asp?descript=jac-creaca-salaj-biserica-rupestra-de-la-jac-pemnita-monului-cod-sit-ran-140734.07 (accessed on 21 July 2024).
43. Atlas, R.M. *Handbook of Microbiological Media*; CRC Press: Boca Raton, FL, USA, 2010.
44. Richmond, J.Y.; McKinney, R.W. *Biosafety in Microbiological and Biomedical Laboratories*; US Government Printing Office: Washington, DC, USA, 2009.
45. Delegou, E.; Karapiperis, C.; Hilioti, Z.; Chasapi, A.; Valasiadis, D.; Alexandridou, A.; Rihani, V.; Kroustalaki, M.; Bris, T.; Ouzounis, C.; et al. Metagenomics of the built cultural heritage: Microbiota characterization of the building materials of the holy aedicule of the holy sepulchre in Jerusalem. *Scient. Cult.* **2022**, *8*, 59–83.
46. Dott, R.H. Wacke, Graywacke and Matrix; What Approach to Immature Sandstone Classification? *J. Sediment. Res.* **1964**, *34*, 625–632. [CrossRef]
47. Folk, R.L. *Petrology of Sedimentary Rocks*; Hemphill Pub. Co.: Austin, TX, USA, 1980.
48. Pettijohn, F.J.; Potter, P.E.; Siever, R. *Sand and Sandstone*; Springer Science & Business Media: Berlin/Heidelberg, Germany, 1987; ISBN 9780387963501.
49. Buzgar, N.; Apopei, A.I.; Diaconu, V.; Buzatu, A. *The Composition and Source of the Raw Material of Two Stone Axes of Late Bronze Age from Neamt County (Romania)—A Raman Study*; Analele Stiintifice de Universitatii AI Cuza din Iasi. Sect. 2, Geologie: Iasi, Romania, 2013; Volume 59, pp. 5–22.
50. Zhang, G.; Gong, C.; Gu, J.; Katayama, Y.; Someya, T.; Gu, J.-D. Biochemical Reactions and Mechanisms Involved in the Biodeterioration of Stone World Cultural Heritage under the Tropical Climate Conditions. *Int. Biodeterior. Biodegrad.* **2019**, *143*, 104723. [CrossRef]
51. Lafuente, B.; Downs, R.T.; Yang, H.; Stone, N. The power of databases: The RRUFF project. In *Highlights in Mineralogical Crystallography*; Armbruster, T., Danisi, R.M., Eds.; De Gruyter: Berlin, Germany, 2015; pp. 1–30. [CrossRef]
52. Norby, P. Synchrotron Powder Diffraction Using Imaging Plates: Crystal Structure Determination and Rietveld Refinement. *J. Appl. Crystallogr.* **1997**, *30*, 21–30. [CrossRef]
53. Magdefrau, E.; Hofmann, U. Biotite, $H_4K_2Mg_6Al_2Si_6O_{24}$. *Z. Kristallogr.* **1937**, *98*, 2–57.
54. Neder, R.B.; Burghammer, M.; Grasl, T.H.; Schulz, H.; Bram, A.; Fiedler, S. Refinement of the Kaolinite Structure From Single-Crystal Synchrotron Data. *Clays Clay Miner.* **1999**, *47*, 487–494. [CrossRef]
55. Cuzman, O.A.; Tiano, P.; Ventura, S. Biodiversity on Stone Artifacts, Chapters. In *The Importance of Biological Interactions in the Study of Biodiversity*; Lopez-Pujol, J., Ed.; IntechOpen: Rijeka, Croatia, 2011.

56. ICOM-CC. Environmental Guidelines ICOM-CC and IIC Declaration. 2014. Available online: https://www.icom-cc.org/en/environmental-guidelines-icom-cc-and-iic-declaration (accessed on 21 July 2024).
57. Šebela, S.; Baker, G.; Luke, B. Cave Temperature and Management Implications in Lehman Caves, Great Basin National Park, USA. *Geoheritage* **2019**, *11*, 1163–1175. [CrossRef]
58. Kukuljan, L.; Gabrovšek, F.; Covington, M.D.; Johnston, V.E. CO_2 Dynamics and Heterogeneity in a Cave Atmosphere: Role of Ventilation Patterns and Airflow Pathways. *Theor. Appl. Climatol.* **2021**, *146*, 91–109. [CrossRef]
59. Mattey, D.; Atkinson, T.; Barker, J.; Fisher, R.; Latin, J.; Durrell, R.; Ainsworth, M. Carbon dioxide, ground air and carbon cycling in Gibraltar karst. *Geochim. Et Cosmochim. Acta* **2016**, *184*, 88–113. [CrossRef]
60. Bergel, S.; Carlson, P.; Larson, T.; Wood, C.; Johnson, K.; Banner, J.; Breecker, D. Constraining the subsoil carbon source to cave-air CO 2 and speleothem calcite in central Texas. *Geochim. Et Cosmochim. Acta* **2017**, *217*, 112–127. [CrossRef]
61. Liu, J.; Zhang, D.; Zhou, G.; Faivre-vuillin, B.; Deng, Q.; Wang, C. CO_2 Enrichment Increases Nutrient Leaching from Model Forest Ecosystems in Subtropical China. *Biogeosciences* **2008**, *5*, 1783–1795. [CrossRef]
62. Tao, C.; Peng, Y.; Zhang, Q.; Zhang, Y.; Gong, B.; Wang, Q.; Wang, W. Diagnosing ozone–NOx–VOC–aerosol Sensitivity and Uncovering Causes of Urban–nonurban Discrepancies in Shandong, China, Using Transformer-Based Estimations. *Atmos. Chem. Phys.* **2024**, *24*, 4177–4192. [CrossRef]
63. Gao, X.; Wang, Y.; Wu, L.; Zheng, F.; Sun, N.; Liu, G.; Liu, Y.; Meng, P.; Sun, L.; Jing, B. The Impact of Anthropogenic VOC Emissions on Atmospheric Pollution: A Case Study of a Typical Industrialized Area in China. *Atmosphere* **2023**, *14*, 1586. [CrossRef]
64. Zerboni, A.; Villa, F.; Wu, Y.-L.; Solomon, T.; Trentini, A.; Rizzi, A.; Cappitelli, F.; Gallinaro, M. The Sustainability of Rock Art: Preservation and Research. *Sustain. Sci. Pract. Policy* **2022**, *14*, 6305. [CrossRef]
65. CCAH. Available online: https://ccaha.org/resources/light-exposure-artifacts-exhibition (accessed on 21 July 2024).
66. Pasanen, A.-L.; Kalliokoski, P.; Pasanen, P.; Jantunen, M.J.; Nevalainen, A. Laboratory Studies on the Relationship between Fungal Growth and Atmospheric Temperature and Humidity. *Environ. Int.* **1991**, *17*, 225–228. [CrossRef]
67. Jain, A.; Bhadauria, S.; Kumar, V.; Chauhan, R.S. Biodeterioration of Sandstone under the Influence of Different Humidity Levels in Laboratory Conditions. *Build. Environ.* **2009**, *44*, 1276–1284. [CrossRef]
68. Taniwaki, M.H.; Hocking, A.D.; Pitt, J.I.; Fleet, G.H. Growth and Mycotoxin Production by Food Spoilage Fungi under High Carbon Dioxide and Low Oxygen Atmospheres. *Int. J. Food Microbiol.* **2009**, *132*, 100–108. [CrossRef] [PubMed]
69. Garaga, R.; Avinash, C.K.R.; Kota, S. Seasonal variation of airborne allergenic fungal spores in ambient PM10—A study in Guwahati, the largest city of north-east India. *Air Qual. Atmos. Health* **2018**, *12*, 11–20. [CrossRef]
70. Korpi, A.; Pasanen, A.L.; Pasanen, P. Volatile Compounds Originating from Mixed Microbial Cultures on Building Materials under Various Humidity Conditions. *Appl. Environ. Microbiol.* **1998**, *64*, 2914–2919. [CrossRef]
71. McLaughlin, J.; Knoppel, H.; The ECA (European collaborative action). *Indoor Air Quality and Its Impact on Man*; European Union: Brussels, Belgium, 1995.
72. Porca, E.; Jurado, V.; Martin-Sanchez, P.M.; Hermosín, B.; Bastian, F.; Alabouvette, C.; Saiz-Jimenez, C. Aerobiology: An ecological indicator for early detection and control of fungal outbreaks in caves. *Ecol. Indic.* **2011**, *11*, 1594–1598. [CrossRef]
73. Ogórek, R.; Lejman, A.; Matkowski, K. Influence of the external environment on airborne fungi isolated from a cave. *Pol. J. Environ. Stud.* **2014**, *23*, 435–440.
74. Pusz, W.; Król, M.; Zwijacz-Kozica, T. Airborne fungi as indicators of ecosystem disturbance: An example from selected Tatra Mountains caves (Poland). *Aerobiologia* **2018**, *34*, 111–118. [CrossRef]
75. Ogórek, R. Fungal Communities on Rock Surfaces in Demänovská Ice Cave and Demänovská Cave of Liberty (Slovakia). *Geomicrobiol. J.* **2018**, *35*, 266–276. [CrossRef]
76. Stupar, M.; Savković, Ž.; Popović, S.; Simić, G.S.; Grbić, M.L. Speleomycology of Air in Stopića Cave (Serbia). *Microb. Ecol.* **2023**, *86*, 2021–2031. [CrossRef] [PubMed]
77. Ogórek, R.; Pusz, W.; Lejman, A.; Uklańska-Pusz, C. Microclimate effects on number and distribution of fungi in the Włodarz underground complex in the Owl Mountains (Góry Sowie), Poland. *J. Cave Karst Stud.* **2014**, *76*, 146–153. [CrossRef]
78. Mohamed, S.; Eid Ibrahim, S. Characterization and Management of Fungal Deterioration of Ancient Limestone at Different Sites along Egypt. *Egypt. J. Microbiol.* **2018**, *53*, 177–191. [CrossRef]
79. Ahmed, E.A.-E.; Mohamed, R.M. Bacterial Deterioration in the Limestone Minaret of Prince Muhammad and Suggested Treatment Methods, Akhmim, Egypt. *Geomaterials* **2022**, *12*, 37–58. [CrossRef]
80. De la Rosa-García, S.C.; Ortega-Morales, O.; Gaylarde, C.C.; Beltrán-García, M.; Quintana-Owen, P.; Reyes-Estebanez, M. Influence of Fungi in the Weathering of Limestone of Mayan Monuments. *Rev. Mex. Mic* **2011**, *33*, 43–51.
81. Abdel Ghany, T.M.; Omar, A.M.; Elwkeel, F.M.; Al Abboud, M.A.; Alawlaqi, M.M. Fungal Deterioration of Limestone False-Door Monument. *Heliyon* **2019**, *5*, e02673. [CrossRef]
82. Singh, P.K.; Ahalavat, A.K.; Vimala, Y. Jatropha curcas, Pongamia pinnata Plantation with Glycine max as Safe and Potent Green Energy Source. *Ann. Plant Sci.* **2014**, *2*, 520–523.
83. Savković, Ž.; Stupar, M.; Unković, N.; Knežević, A.; Vukojević, J.; Grbić, M.L. Fungal Deterioration of Cultural Heritage Objects. In *Biodegradation Technology of Organic and Inorganic Pollutants*; IntechOpen: London, UK, 2021.
84. De Leo, F.; Urzì, C.; de Hoog, G.S. New Meristematic Fungus, Pseudotaeniolina globosa. *Antonie Van Leeuwenhoek* **2003**, *83*, 351–360. [CrossRef]

85. Gorbushina, A.A.; Krumbein, W.E.; Hamman, C.H.; Panina, L.; Soukharjevski, S.; Wollenzien, U. Role of Black Fungi in Color Change and Biodeterioration of Antique Marbles. *Geomicrobiol. J.* **1993**, *11*, 205–221. [CrossRef]
86. Wollenzien, U.; de Hoog, G.S.; Krumbein, W.E.; Urzí, C. On the Isolation of Microcolonial Fungi Occurring on and in Marble and Other Calcareous Rocks. *Sci. Total Environ.* **1995**, *167*, 287–294. [CrossRef]
87. Dornieden, T.; Gorbushina, A.A.; Krumbein, W.E. Physical and Chemical Interactions of Sub-aerial Biofilms with Objects of Art. In *Of Microbes and Art: The Role of Microbial Communities in the Degradation and Protection of Cultural Heritage*; Ciferri, O., Tiano, P., Mastromei, G., Eds.; Springer: Boston, MA, USA, 2000; pp. 105–119.
88. Warscheid, T.; Braams, J. Biodeterioration of Stone: A Review. *Int. Biodeterior. Biodegrad.* **2000**, *46*, 343–368. [CrossRef]
89. Berner, M.; Wanner, G.; Lubitz, W. A Comparative Study of the Fungal Flora Present in Medieval Wall Paintings in the Chapel of the Castle Herberstein and in the Parish Church of St Georgen in Styria, Austria. *Int. Biodeterior. Biodegrad.* **1997**, *40*, 53–61. [CrossRef]
90. Romero, S.M.; Giudicessi, S.L.; Vitale, R.G. Is the Fungus Aspergillus a Threat to Cultural Heritage? *J. Cult. Herit.* **2021**, *51*, 107–124. [CrossRef]